

AD-A258 706

2



PL-TR-92-2079

OBSERVATION OF IONOSPHERIC MODIFICATION USING HIGH POWER OBLIQUE HF TRANSMISSIONS

Gary S. Sales
Yuming Huang

DTIC

OCT 5 1992

University of Massachusetts, Lowell
Center of Atmospheric Research
450 Aiken Street
Lowell, MA 01854

June 1992

Scientific Report No. 1

APPROVED FOR PUBLIC RELEASE; DISTRIBUTION UNLIMITED



PHILLIPS LABORATORY
AIR FORCE SYSTEMS COMMAND
HANSOM AIR FORCE BASE, MASSACHUSETTS 01731-5000

92-26388




3788

92 10 2 033

This technical report has been reviewed and is approved for publication.


JOHN L. HECKSCHER
Contract Manager


JOHN E. RASMUSSEN
Branch Chief


WILLIAM K. VICKERY
Division Director

This document has been reviewed by the ESD Public Affairs Office (PA) and is releasable to the National Technical Information Service (NTIS).

Qualified requestors may obtain additional copies from the Defense Technical Information Center. All others should apply to the National Technical Information Service.

If your address has changed, or if you wish to be removed from the mailing list, or if the addressee is no longer employed by your organization, please notify PL/TSL, Hanscom AFB, MA 01731-5000. This will assist us in maintaining a current mailing list.

Do not return copies of this report unless contractual obligations or notices on a specific document require that it be returned.

REPORT DOCUMENTATION PAGE			Form Approved OMB No. 0704-0188	
<small>Public reporting burden for this collection of information is estimated to average 1 hour per response, including the time for reviewing instructions, searching existing data sources, gathering and maintaining the data needed, and completing and reviewing the collection of information. Send comments regarding this burden estimate or any other aspect of this collection of information, including suggestions for reducing this burden, to Washington Headquarters Services, Directorate for Information Operations and Reports, 1215 Jefferson Davis Highway, Suite 1204, Arlington, VA 22202-4302, and to the Office of Management and Budget, Paperwork Reduction Project (0704-0188), Washington, DC 20503.</small>				
1. AGENCY USE ONLY (Leave blank)		2. REPORT DATE June 1992	3. REPORT TYPE AND DATES COVERED Scientific Report No. 1	
4. TITLE AND SUBTITLE Observation of Ionospheric Modification Using High Power Oblique HF Transmissions			5. FUNDING NUMBERS PE 62101F PR 4643 TA 10 WU AQ	
6. AUTHOR(S) Gary S. Sales and Yuming Huang			Contract F19628-90-K-0039	
7. PERFORMING ORGANIZATION NAME(S) AND ADDRESS(ES) University of Massachusetts Lowell Center for Atmospheric Research 450 Aiken Street Lowell, MA 01854			8. PERFORMING ORGANIZATION REPORT NUMBER	
9. SPONSORING / MONITORING AGENCY NAME(S) AND ADDRESS(ES) Phillips Laboratory Hanscom AFB, MA 01731-5000 Contract Manager: John Heckscher/GPID			10. SPONSORING / MONITORING AGENCY REPORT NUMBER PL-TR-92-2079	
11. SUPPLEMENTARY NOTES				
12a. DISTRIBUTION / AVAILABILITY STATEMENT Approved for public release; distribution unlimited			12b. DISTRIBUTION CODE	
13. ABSTRACT (Maximum 200 words) A series of experiments were carried out during late May 1991 to investigate changes produced in the ionosphere by a high power HF transmitter operating at a frequency approximately two times the F-layer critical frequency. These high power oblique transmissions heated a region of the ionosphere some 1200km east of the Delano, CA Voice of America relay station, operating with an effective radiated power of 90 dBW. An HF probe signal was used to detect changes in the ionosphere as it passed through the modified region. The probe system, operating at a frequency very close to the heater frequency, frequently showed amplitude changes that correlate well with the ten minute on/off cycling of the high power transmitter. This preliminary study used several signal processing methods to detect these changes in the presence of strong polarization fading. The results indicate that the amplitude of the probe signal decreased by 2 to 3 dB, often within 15 to 30s after the high power transmitter was turned on.				
14. SUBJECT TERMS HF Propagation, High Power HF Systems, Ionospheric Modification, Oblique Propagation, Signal Processing			15. NUMBER OF PAGES 38	
			16. PRICE CODE	
17. SECURITY CLASSIFICATION OF REPORT Unclassified	18. SECURITY CLASSIFICATION OF THIS PAGE Unclassified	19. SECURITY CLASSIFICATION OF ABSTRACT Unclassified	20. LIMITATION OF ABSTRACT SAR	

TABLE OF CONTENTS

	Page
1.0 INTRODUCTION	1
1.1 High Power Transmitter Phasing.....	6
2.0 DATA PROCESSING AND ANALYSIS.....	6
2.1 Amplitude Data.....	6
2.2 Cross-Correlation Analysis.....	13
2.3 Spectrum Analysis.....	16
3.0 RAY TRACING.....	18
4.0 IONOSPHERIC HEATING.....	21
4.1 Introduction.....	21
4.2 Nighttime E-region Heating.....	25
5.0 SUMMARY.....	28
REFERENCES	31

Acquisition Form
 TITLE: ☐ ☒ ☐
 DTIC FILE: ☐ ☒ ☐
 DATE OF ACQ: ☐ ☒ ☐
 ACQUISITION: ☐ ☒ ☐

A-1

LIST OF FIGURES

Figure No.		Page
1	Structure of Heated Region Using Sample Ray Tracing	2
2	Illustration of the Movement of the Heated Region.....	4
3	Amplitude Data Showing Typical Fading.....	8
4	Amplitude Data for the Three Selected Periods.....	10
5	MUF Curves and Heater Frequencies for the Selected Data Samples.....	11
6	Superimposed Epoch for Selected Amplitude Data.....	12
7	Ray Tracings for Selected Data Periods.....	14
8	Amplitude Probability Distribution for the Selected Data Periods for the Transmitter On and Off Intervals.....	15
9	Cross-Correlation for the Selected Data	17
10.	Fourier Spectra for the Selected Data Samples.....	19
11.	Ray Tracings Illustrating the Movement of the Caustic Region.....	20
12.	Scaled foEs and hEs for 26 May 1992	27
13.	Increased Absorption for Sporadic-E ionization (night)	29

LIST OF TABLES

Table No.		Page
1	Temperature Change (%) vs. Altitude.....	23

1.0 INTRODUCTION

During the period May 25 to June 1, 1991 ionospheric modification experiments (IONMOD) were conducted using the VOA high power (effective radiated power = 90 dBW) transmitting facility at Delano, CA. An oblique propagation path from Delano, CA to Shreveport, LA, a distance of 2400 km, was established for probing the heated region. Only when the VOA transmitter operated at or near 12 MHz was the full power capability of the Delano facility achieved. For this reason, the frequency of choice for these experiments was 12 MHz, particularly at night when the MUF(2400) was close to 12 MHz. With a fixed heating frequency, the position of the maximum heating was allowed to vary as the ionospheric conditions changed during the experiments. This report discusses the approximately 30 hours of nighttime data accumulated during the test period. The small amount of daytime data (approximately 10 hours) will be analyzed later.

Heating occurs where the high field strengths from the powerful transmitter interact with the ambient electrons in the plasma. The heating process is effective only where there are sufficient collisions between the electrons and the neutral atoms and molecules. Two separated regions are considered where this heating process may take place. First, in the F-region, where the caustic focusing of the rays in the reflection area results in an increased field intensity above what is expected on the basis of inverse square spreading losses. However, in the F-layer, at night, when the reflection is above 300 km, the electron collision frequency is very small and it is very difficult to change the electron temperature. On the other hand, at night there exists a weak E-layer near 100 km with an estimated $f_oE = 0.6$ MHz and sporadic E (Es) with f_oEs around 3 MHz and at times even greater. Here, because the collision frequency is much larger and the spreading loss is less (the range to the E-region at 12° elevation is ≈ 400 km while the range to the F-region caustic is ≈ 1400 km), the heating is considerably more effective.

The ray structure at a VOA frequency of 12 MHz is illustrated in Figure 1 using an analytical ray tracing program and a typical nighttime electron density profile. The high density of rays near the apogee in the F-layer reflection region represents the focusing of the radio energy and indicates the region where the local electric field strength is intensified after reflection. This region of enhanced field strength is

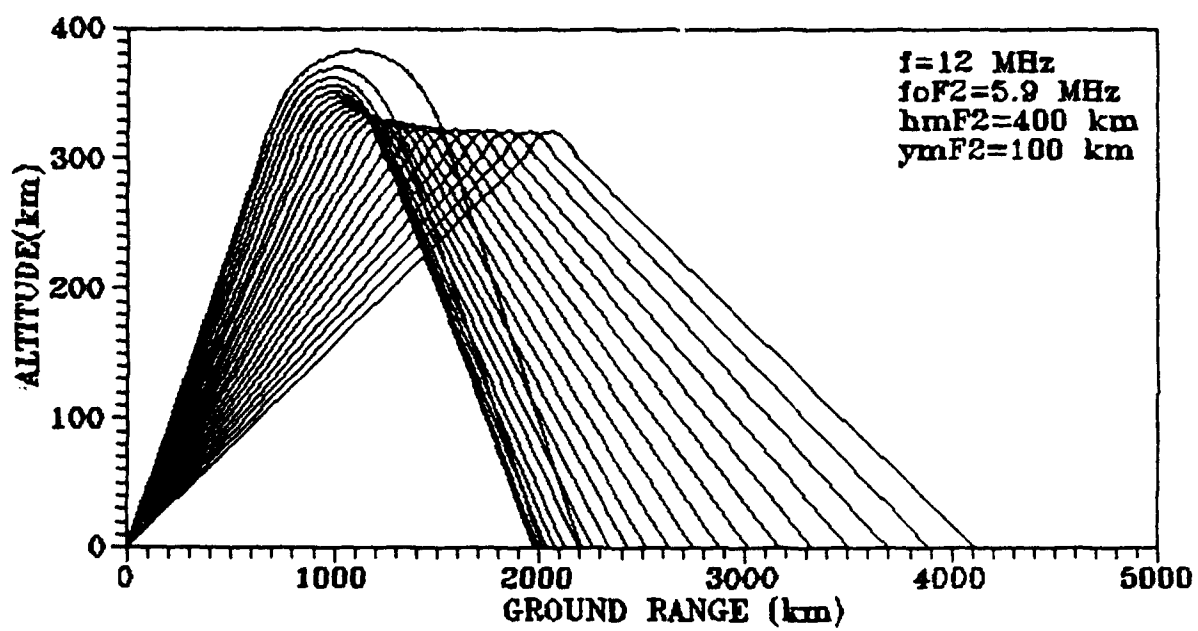


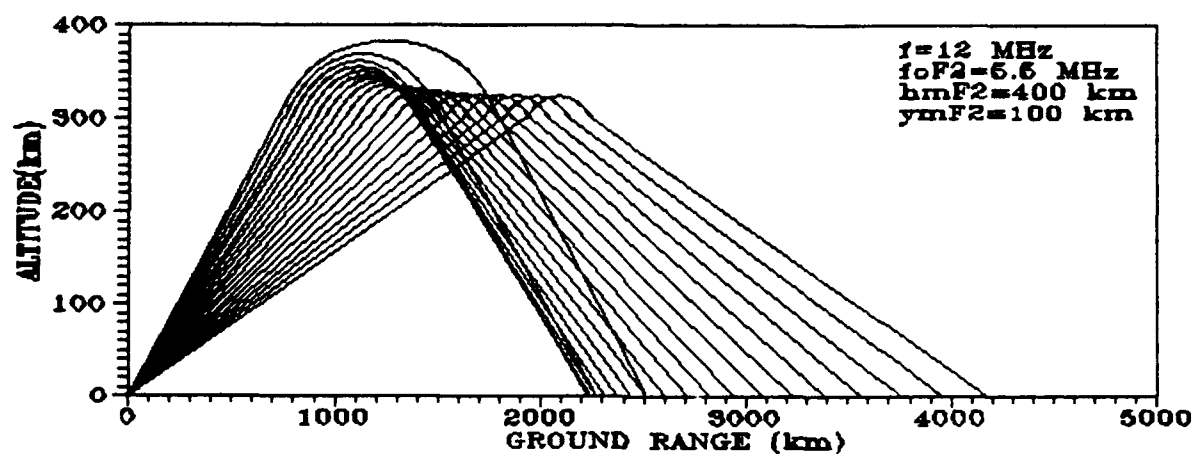
Figure 1. Structure of Heated Region Using Sample Ray Tracing

one of the areas where ionospheric heating in the F-region is expected (E. Field and R. Bloom., 1989). A second area, that is also a likely location of ionospheric heating, is in the E-region (80 to 120 km) in spite of the fact that there is no ray focusing. Here, it will be shown later, that because of the proximity of the layer to the heater, the field intensity of the heater wave is sufficiently strong to produce heating without forming a caustic region.

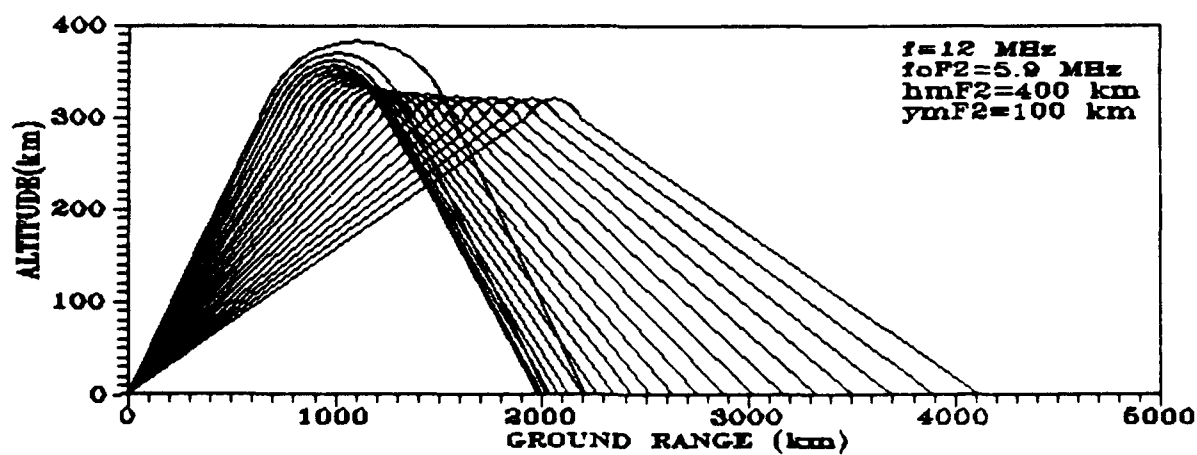
For a particular path, in this experiment from Delano, CA. to Shreveport, LA. a distance of 2400 km, the antenna pattern of the VOA 2-D curtain array was steered vertically so as to place the maximum radiated power density near the midpath area at the ray focusing region (caustic) illustrated in Figure 1. Based on the earlier analyses (Field et al., 1989; Sales, G. et al., 1990), the VOA frequency should always lie just below the maximum useable frequency (MUF) for the particular oblique path insuring that a probe signal passes through the maximum heated region. The high gain VOA antenna, steerable in azimuth and elevation, was directed to an azimuth of 91 degrees relative to true north, boresighted on Shreveport, LA and at an elevation angle consistent with the illumination of the caustic heating region above Albuquerque, NM, halfway along the path from Delano to Shreveport.

To determine the effects of heating on the ionosphere, a second transmitter, a low power "probe" system (500 W), was located at the VOA facility at Delano and operated at a different frequency to that of the VOA transmitter (typically 100 to 500 kHz away from the heater frequency). The probe signal was received at Barksdale AFB, Shreveport, LA., 2400 km away. Using a probe frequency close to that of VOA heater frequency ensures that the probe rays pass through or close to the heated volume resulting from the high power VOA transmissions.

The high power signal operated with a 10 minute period (5 minutes off and 5 minutes on) and changes in the probe signal which is on continuously, was determined by post processing the digitally recorded data from each of three receive antennas. Since VOA operates only at specific frequencies within the international broadcast bands, it was not always possible to select an operating frequency just below the MUF. Using the analytic ray tracing program, for ionospheric layers with different f_oF_2 's and maximum heights, two ray configurations are shown in Figure 2. In Figure 2a, the f_{heat} is close to the MUF and the rays from Delano, CA to Shreveport, LA (2400 km) pass through the E-layer heated region near an altitude of



(a) Ray Tracing $MUF = f_{HTR}$



(b) Ray Tracing $MUF = f_{HTR} + 1.5$ MHz

Figure 2. Illustration of the Movement of the Heated Region

100 km and then through the F-layer caustic region formed by the VOA rays. Figure 2b represents the situation when the same heater frequency is approximately 1.5 MHz below the maximum useable frequency MUF(2400) for the same path. Tracing these rays back from Barksdale indicates that the probe signal once again passes through the illuminated E-region but only through the weaker part of the caustic formed by the skip rays, and not through the "main" focusing region. The details of these situations are discussed later in the report.

In addition to the probe system, a Digisonde 256 vertical ionospheric sounder operated near the mid-point (1200 km) of the propagation path at Kirtland AFB, Albuquerque, NM. The Digisonde was used for frequency and elevation angle management of the VOA high power transmitting system as well as a diagnostic tool to detect changes in the overhead ionosphere that might be associated with the heating process.

For frequency management, vertical incidence ionograms were usually taken every 15 minutes (sometimes every one minute, depending on the particular experimental objective), scaled and then used, with transmission curve overlays to determine the MUF for 2400 km for both the VOA and the probe signals. Between sequential vertical incident ionograms, each normally taking one minute to complete, the Digisonde operated in the drift mode (fixed frequency), to map the distribution of ionospheric reflection sources over a large area, some with a radius of 300 km centered on the sounder site. Such reflection sources indicate the presence of a medium scale (100 km) irregularities in the F-region, and when the locations of these sources, plotted on a polar graph results in a "sky map" of the detected ionospheric reflection sources. These skymap measurements were designed to detect the formation of F-region ionospheric instabilities generated by the high power heater. The Digisonde vertical soundings and skymaps are not greatly effected by the MUF/ f_{heater} variations. The sounder responds only to reflection sources at zenith angles of up to ± 45 degrees, which is sufficient to follow any changes in the F-layer heated region but not in the E-region disturbed area which lies out of the field of view of the sounder; some 700 km closer to Delano.

The F-region skymaps from the heating experiments were examined and they showed no changes that correlate with the heater cycling. Initially, this was puzzling, but as is shown later, if the major heating was not in the F-layer near

overhead at the midpath point but in the E-layer, far removed from the vertical sounding, then this negative result is not so surprising.

Ray tracings carried out at the field site during these experiments showed that the required elevation angles for illuminating the reflection region was about 12° and did not vary greatly as the ionosphere changed. For this reason the elevation angle was selected using the available antenna patterns and was not changed for all the nighttime measurement periods.

1.1 High Power Transmitter Phasing

In past experiments, there has been some doubt as to whether the three VOA transmitters were correctly phased relative to each other to achieve maximum radiated power. During these experiments a system of phasing, developed by J. Heckscher, Phillips Laboratory, uses signal amplitude nulls, as received down range at Barksdale, to ensure that each of the two outer transmitters are out of phase with the center reference transmitter. With this method, transmitters A and B (C off) were adjusted to give a null at Barksdale, indicating that they were out of phase. After this operation, transmitters B and C were nulled (while A was turned off) in the same manner. At this stage, transmitters A and C are in phase with each other and both are out of phase with the center transmitter B. To put all three transmitters in-phase then only required that the phase of the drive of transmitter B be switched by 180° .

2.0 DATA PROCESSING AND ANALYSIS

2.1 Amplitude Data

All the data processing was carried out after the completion of the experiments. The recorded data consists of the middle 400 spectrum lines centered on zero frequency of the 4096 point Doppler spectrum of the signal as obtained on each of the three antennas of the probe receive array. Most recorded spectra show two strong modes, which have been identified as the high ray and the low ray for the nighttime F-layer propagation mode from Delano to Barksdale. All of the subsequent analysis was carried out using the low ray signal, distinguished from the high ray using the separated Doppler spectrum lines.

The probe data for each of the five nighttime campaigns was processed to determine the amplitude of the dominant low ray mode as a function of time. Dominant is used in the sense that this mode was present almost all of the time with the greater spectrum amplitude. It is immediately apparent (Figure 3) that there is significant fading on the probe channel (all of the subsequent amplitude graphs are measured as relative amplitude corrected for gain adjustments during the experiments and the time scale on these graphs are measured in 15 s. counts beginning at the start of each of the separate files). This type of fading occurs throughout the experiment. This intense fading (often 6 dB or more) makes it difficult to recognize small changes caused by the heating (1 to 2 dB for a 5% depletion of electron density; Sales and Platt, 1988).

During the nighttime measurements, a number of characteristic amplitude changes were often observed that appear to be synchronized with the heater cycling. Three different time periods are analyzed in detail in this preliminary report to illustrate the type of phenomena that have been observed. These selected intervals are:

26 May 1991 0700 to 0730 UT

29 May 1991 0605 to 0705 UT

29 May 1991 0735 to 0815 UT

These data periods are limited to the nighttime when the optimum heating frequency was either 12 MHz or 15 MHz, corresponding to an ERP of 90 dBW and 85 dBW, respectively. Because of focusing in the caustic region, the electric field strength in the ionosphere, at a nominal altitude of 300 km, is greater than the field strength corresponding to inverse square spreading for the rated ERP at a range of 1200 km (203 mV/m). Because the MUF(2400) was often greater than 12 MHz, the range to the heated region was, at times, significantly less than 1200 km. If we assume a 6 dB increase in field strength within the caustic region and an additional 3 dB when the range to the heated region is reduced to 800 km, relative to 1200 km, as the MUF increases, the field strength in the ionosphere approaches 0.5 V/m. In the E-region the field strength, at the same time without focusing, is also about 0.5 V/m.

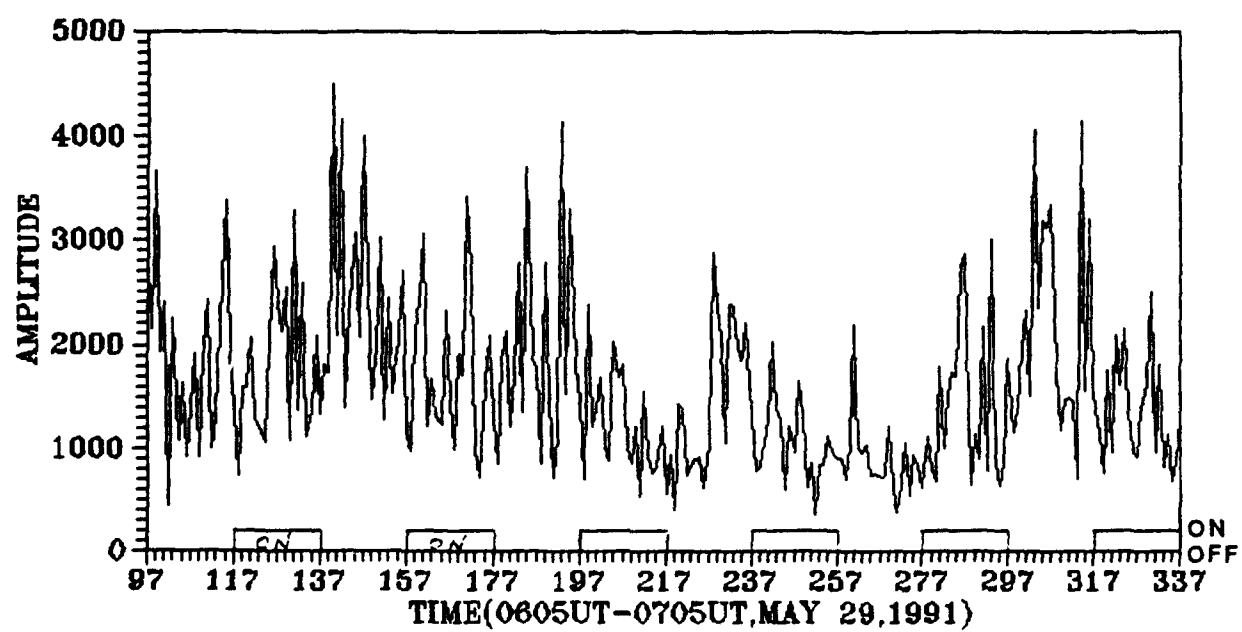


Figure 3. Amplitude Data Showing Typical Fading

The raw amplitude data for the selected periods are shown in Figure 4. Figure 4a is the received amplitude for the period 0700-0730 UT on 26 May 91 when VOA high power transmitter was operating at 11.9 MHz and the probe was operating at 11.545 MHz. For the selected examples the corresponding MUF(2400)'s are shown in Figure 5 for the entire operating period on the same days. Whenever the MUF dropped below the heating frequency, the heater frequency was lowered to insure propagation to the probe receive site. When the MUF exceeded the heater frequency by more than 3 MHz, the heater and probe frequency were both raised. These changes, particularly when the frequency had to be raised, were determined by the available VOA frequencies and often the frequency change had to be delayed until the new higher frequency was below the MUF.

Figure 6 shows the same data as in Figure 4, but where the successive heating cycles for these periods are superimposed on top of each other, using the transition time of heater off to heater on as the reference time. In Figure 6a we see the superposition of three heating cycles. Here the amplitude of the received signals drop rapidly each time the heater is turned-on. From this figure it can be seen that the change in amplitude during these transitions is consistent and relatively large, close to 20%. This superimposed epoch method was used to reduce the obscuring effects of the polarization fading. What remains is a clear indication of the changed amplitude (reduction) following the VOA heater turn on. It should be recognized that the data sampling period is always 15 seconds and changes faster than this are not observable. Figure 6a for 26 May 91 is different from the other two examples, showing what appears to be an apparent recovery of the amplitude after 2 minutes of heating. This effect makes it difficult to compare these data with the other two selected data periods.

On 29 May, 1991, beginning at 0605 UT, six heating cycles are superimposed to better visualize the effects of the high power heater turn-on (Figure 6b). Here, a consistent 10 to 15 % decrease in the amplitude of the probe signal is observed. During this period of one hour, both the heater and the probe operated at frequencies near 12 MHz, while the MUF for the path varied from 14.4 to 15.8 MHz. Finally, the superimposed epoch method is applied to the data set for 29 May 91, 0735 - 0815 UT (Figure 6c) and the amplitude shows similar effects.

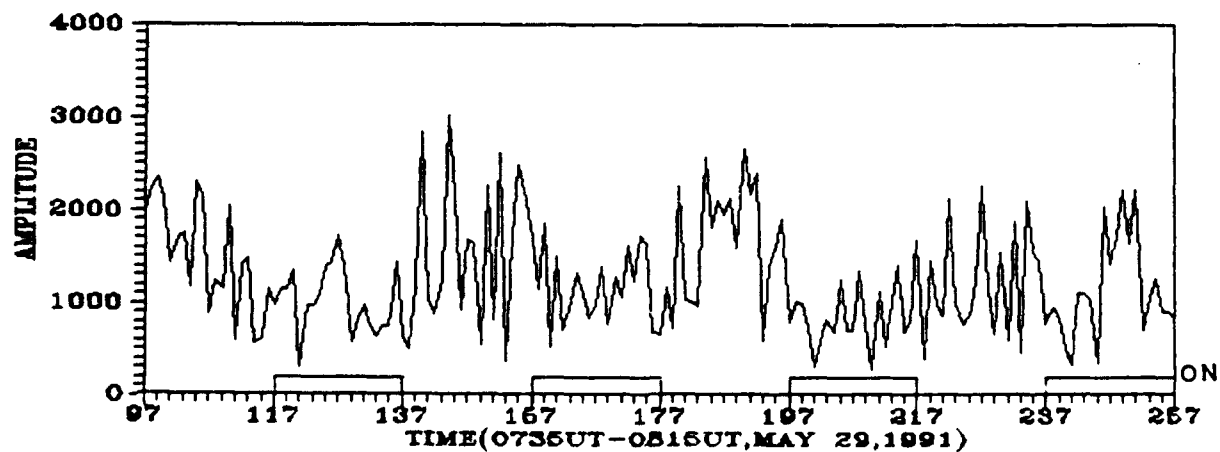
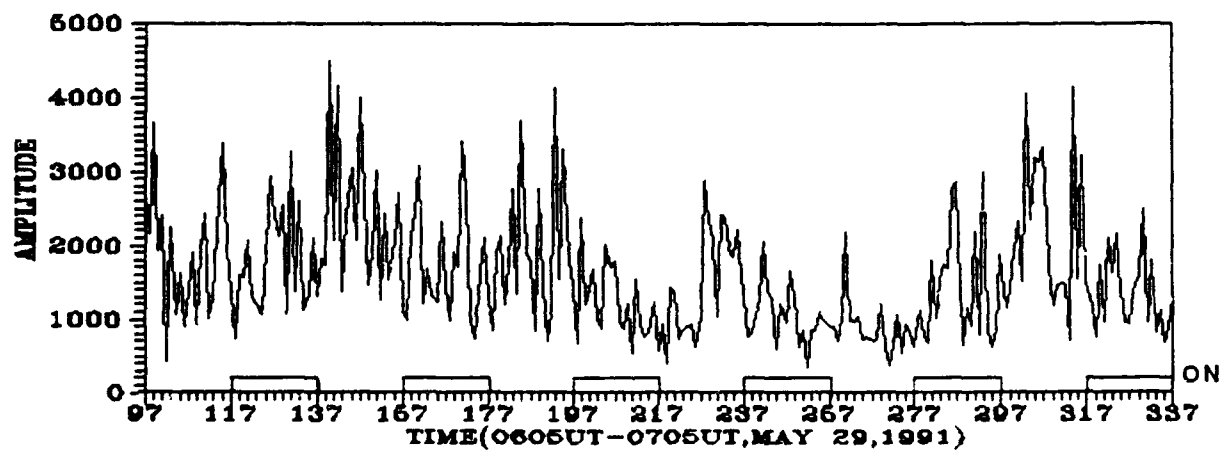
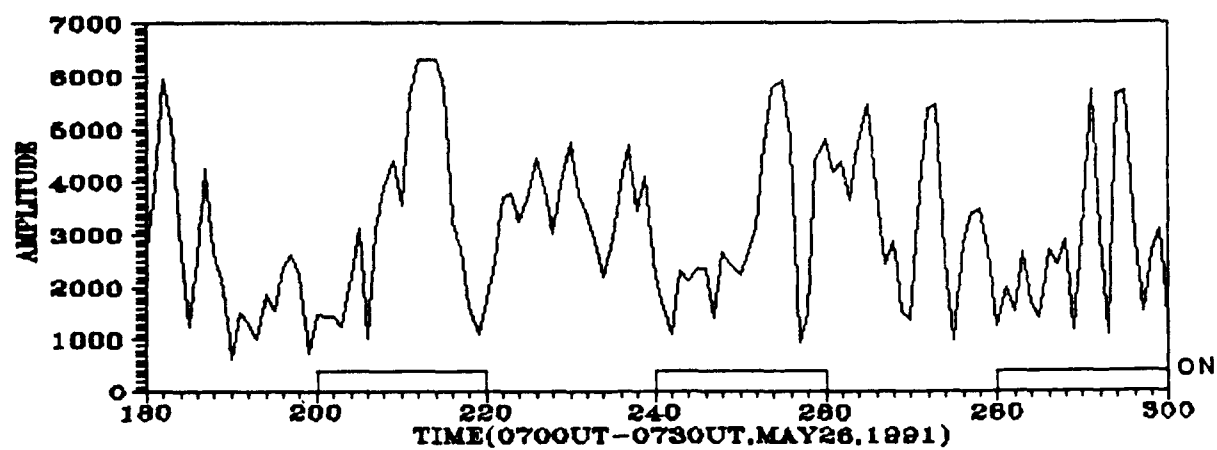


Figure 4. Amplitude Data for the Three Selected Periods

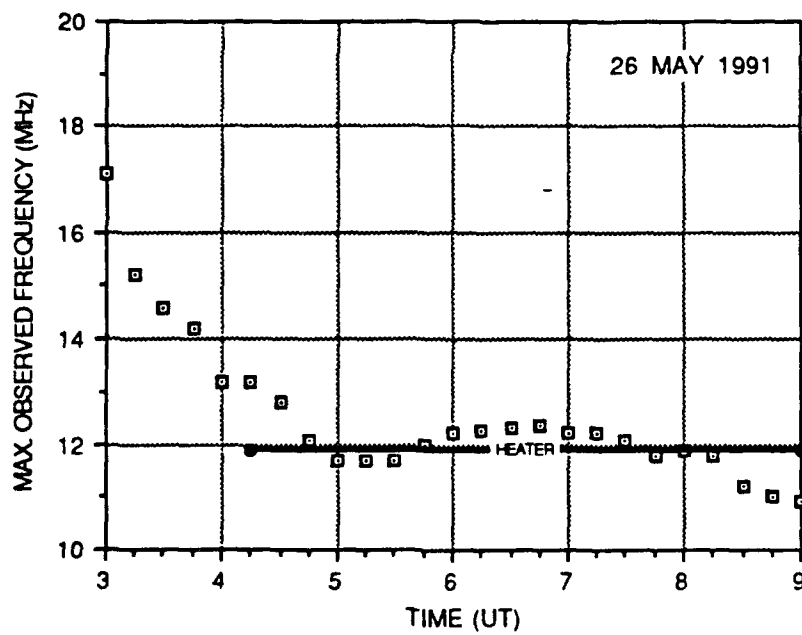
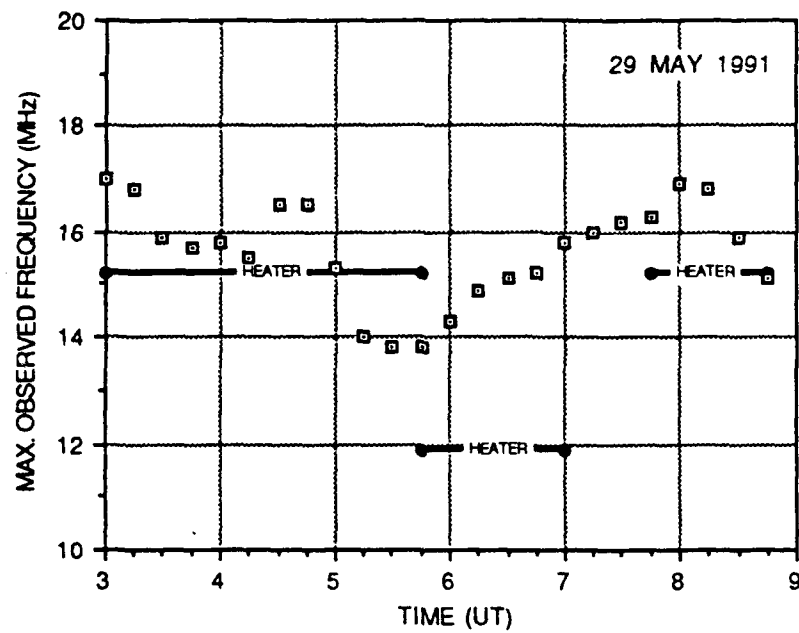


Figure 5. MUF Curves and Heater Frequencies for the Selected Data Samples

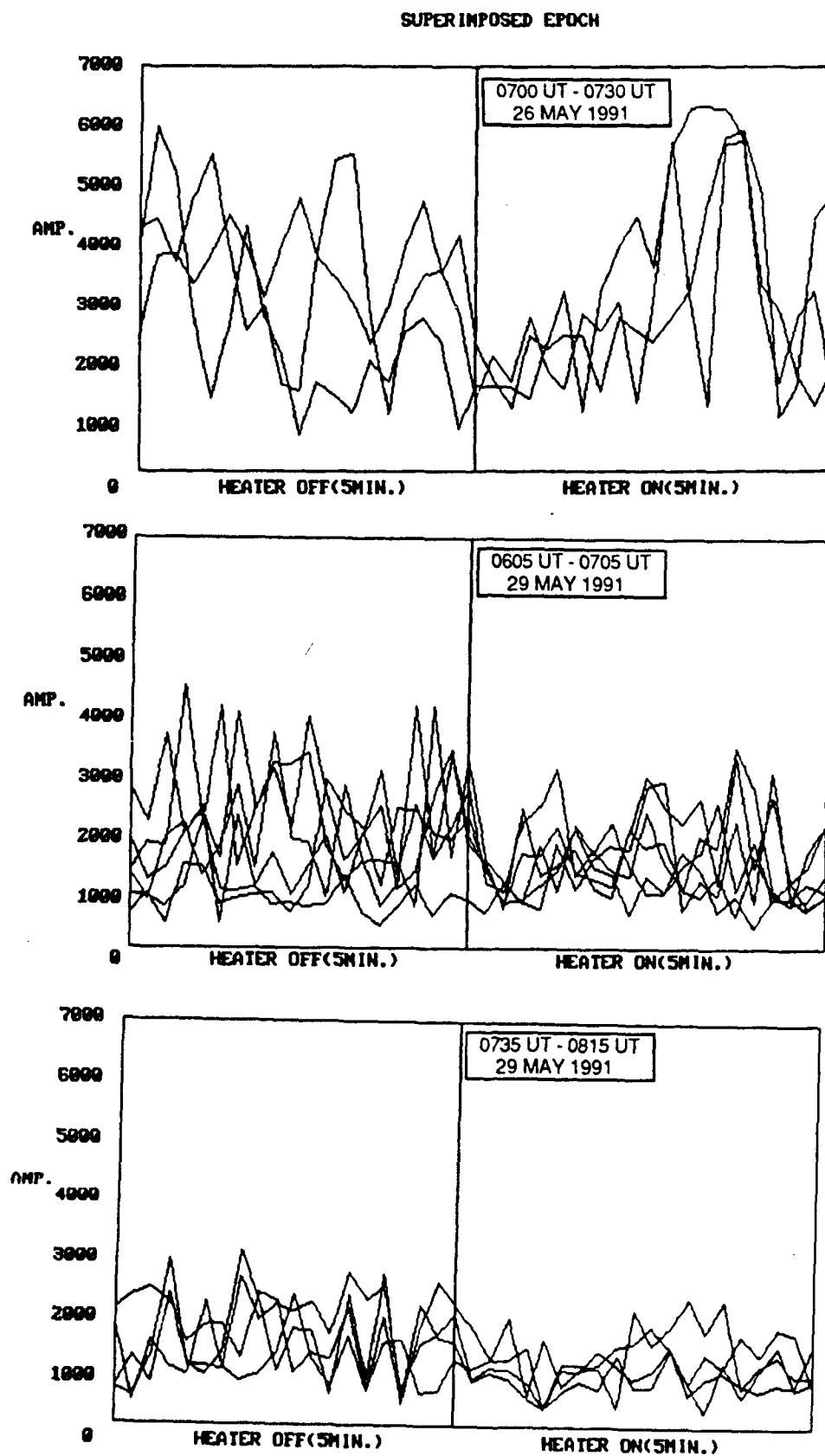


Figure 6. Superimposed Epoch for Selected Amplitude Data

The ray tracings in Figure 7 shows different configurations of the heated region and the probe signal propagating to Shreveport for the 0605-0705 UT 29 May data period. Here, the heater and probe systems both operated on a frequency around 12 MHz while the MUF varied from 14.2 to 15.8 MHz over the selected 60 minute period. The amplitude of the probe signal shows a clear decrease at the time of the heater turn-on. The amplitude change as a result of the heating during these cycles is of the order of 20%. For the 0735-0815 UT 29 May data, the heater operated at 15 MHz, while the MUF was approximately 16.6 MHz.

For these periods, Figure 8 shows separate amplitude distributions for the several interlaced heater-on and heater-off periods. These distributions indicate a convincing decrease in the probability of large amplitudes when the heater is on compared to the off-cycle data during the selected periods. Statistical analysis, using the χ^2 -test, indicates that the probability that these two sample distributions are derived from the same population is very small; less than one chance in 10000.

2.2 Cross-Correlation Analysis

A second method of analysis was developed to present these data in a manner that reduces the effects of the strong fading of the probe signal. Here, the amplitude data is cross-correlated with a square wave that has a duration of 10 minutes corresponding to the heating period. The square wave has an amplitude of +1 representing heater off, for five minutes and then switches to -1, heater on, for the next five minutes. The attempt here is to search for those times when this simple square wave model replicates the changed (reduced) amplitude that corresponds to the turn-on in the heating cycles. Positive and negative peaks in the correlation function $r(j)$ result if the actual amplitude data follows this simplified stepped behavior. The correlation function used here is defined as:

$$r(j) = \frac{\sum_{i=0}^{39} (D_{i+j} - \bar{D}) S_i}{\left[\sum_{i=0}^{39} (D_{i+j} - \bar{D})^2 \sum_{i=0}^{39} S_i^2 \right]^{1/2}}$$

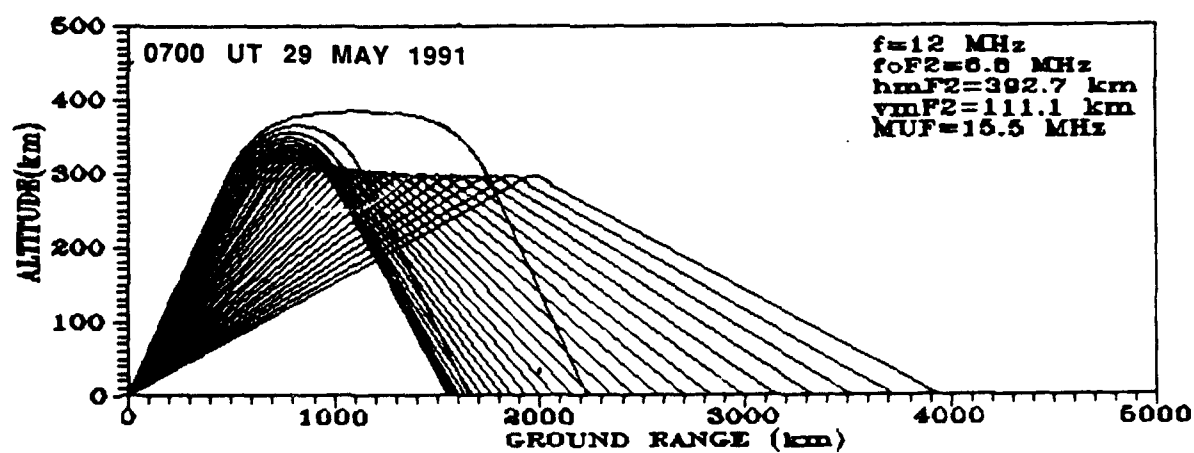
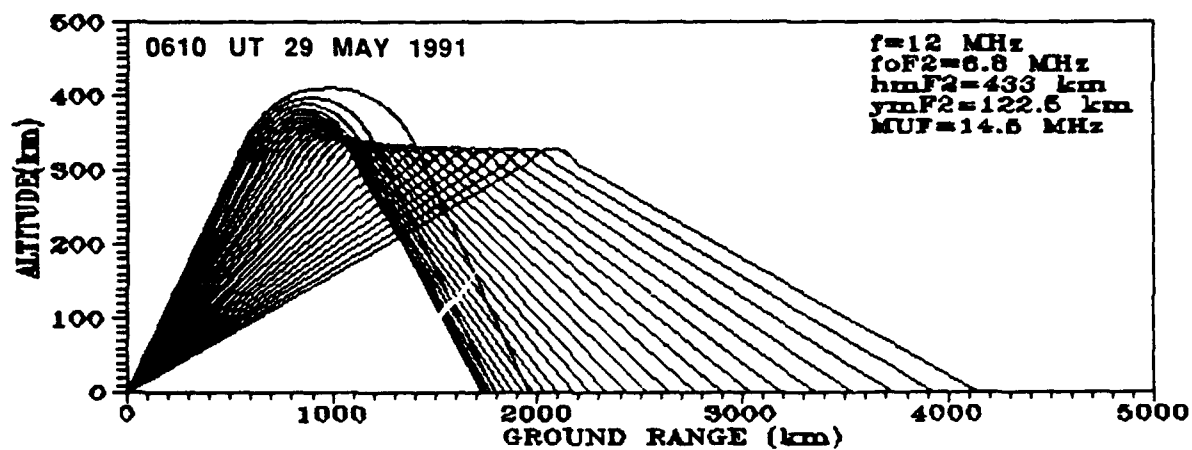


Figure 7. Ray Tracings for Selected Data Periods

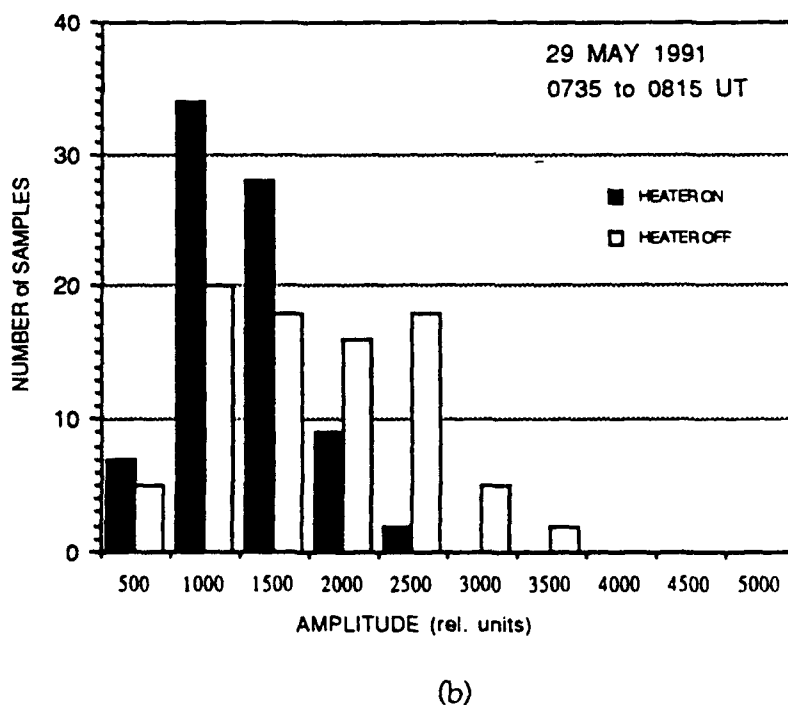
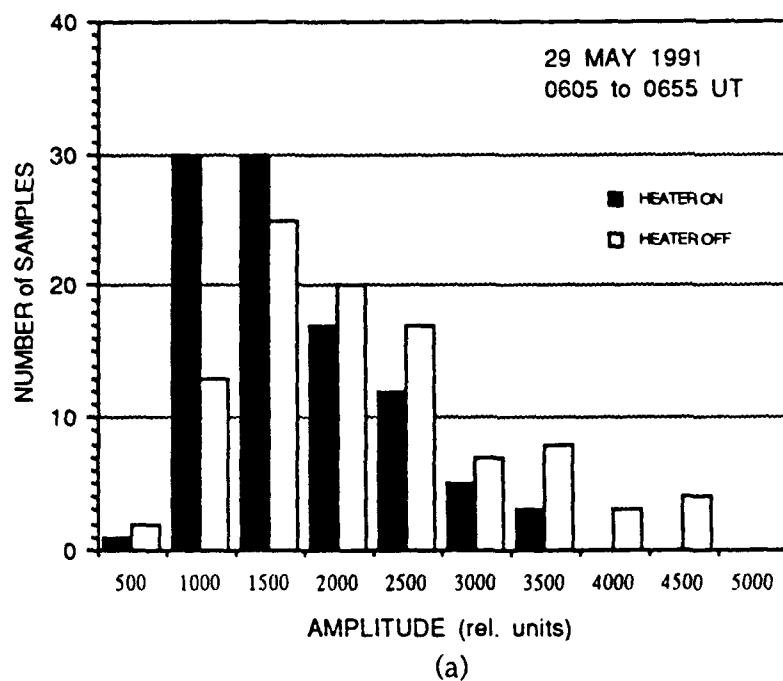


Figure 8. Amplitude Probability Distribution for the Selected Data Periods for the Transmitter On and Off Intervals

where D_{i+j} is the actual amplitude data beginning at the j^{th} point and going on to the $j+40$ point, \bar{D} is the mean data amplitude over the same 40 points and:

$$\begin{aligned} S_i &= +1 && \text{for } i = 0 \text{ to } 19 \\ &&& \text{and} \\ S_i &= -1 && \text{for } i = 20 \text{ to } 39 \end{aligned}$$

When several heating cycles follow each other, this method is particularly effective since the positive and negative correlation peaks will be separated by the 10 minute period (40 points). This technique identifies those cycles where the heating process was secured. This correlation analysis method averages over the rapid amplitude fading and searches for changes in the mean amplitude between adjacent five minute intervals. When no significant amplitude change results from the heating, the cross-correlation is small, i.e., $r \approx 0$.

For the two selected data samples discussed earlier, Figure 9 shows the results of the cross-correlation processing. The cross-correlation method does not work well for the 26 May data since there appears to be a consistently strong amplitude recovery about 2 minutes into the heating period and this variation is not correctly modeled by the simple step function used for the correlation processing. The amplitude variations for the 26 May data sample result in a peak correlation that is not correctly located in terms of the heater off/on cycling as with the other two data samples. However, the strong 10 minute periodicity is still apparent indicating that the heating is the source of the amplitude variations. For the other two data samples, the variations of the cross-correlation are as expected and indicate a mean time lag of less than one minute.

2.3 Spectrum Analysis

Finally, to confirm the presence of the heating period (10 minutes) in the amplitude data, a spectrum analysis of the amplitude samples, spaced 15s apart, was carried out using a Fast Fourier Transform (FFT) method. The amplitude samples used in this analysis are the peak amplitude of the received probe signal spectrum as measured on the reference antenna. From 200 to 256 points (50 to 64 minutes) were selected

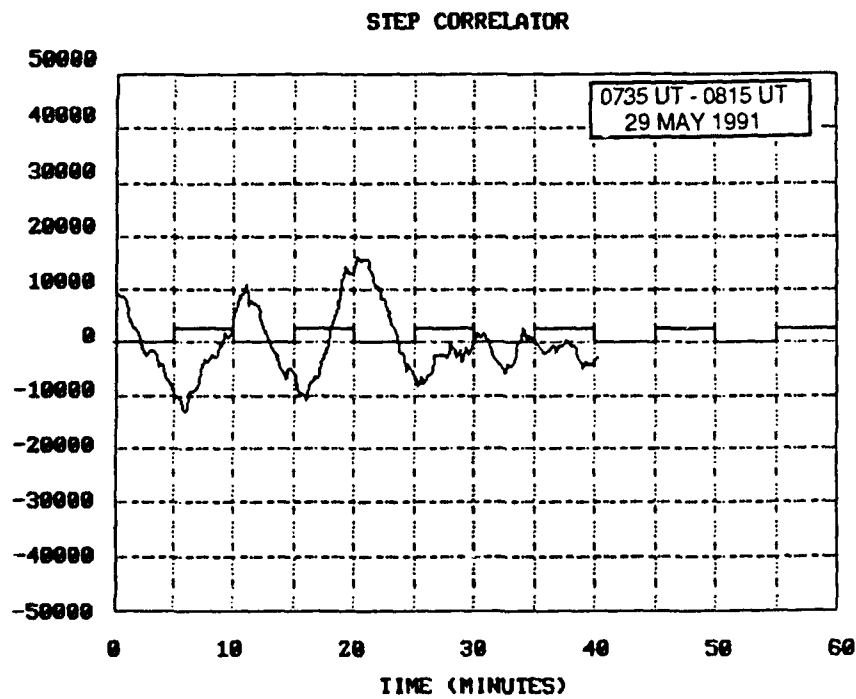
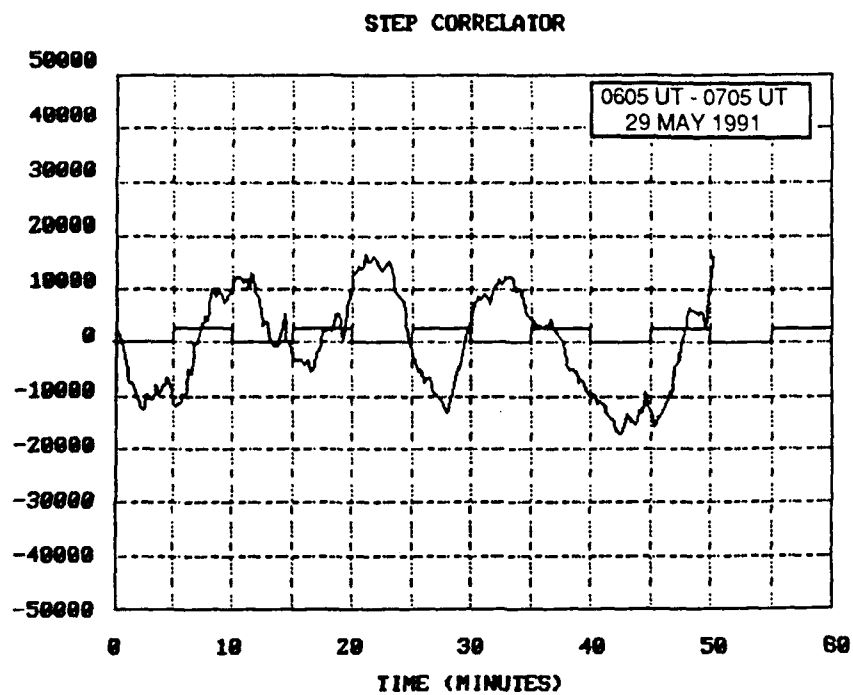


Figure 9. Cross-Correlation for the Selected Data

for the spectrum analysis. When the number of selected points was less than 256, the data was augmented to bring the number to the required 256. This length of data represents between 5 to 6 heating cycles.

These power spectra have a frequency resolution of 0.26 mHz and the 10 minute heating period is equivalent to a frequency of 1.67 mHz, lying between the 6th and 7th line in the computed spectrum. On each of the spectra, the frequency that corresponds to the 10 minute heating cycle, is indicated by a bold vertical line. Figure 10 shows each of the processed spectra with a relatively strong, distinct, component very near the expected heating frequency.

3.0 RAY TRACING

To understand the effects of the powerful heater signal on the low power probe signal, a series of ray tracings have been carried out for a range of electron density profiles corresponding to the changing ambient ionosphere during the heating experiments. These profiles are derived from the vertical soundings made at Kirtland AFB, Albuquerque, NM, near the midpoint of the propagation path from Delano, CA to Shreveport, LA. The MUF curves presented earlier were derived from the same vertical ionograms using the appropriate transmission curve overlays.

These ray tracing were carried out assuming that the heater frequency was 12 MHz. As stated earlier, the 12 MHz heating was used for the great majority of time during these experiments because at that frequency the maximum transmitting antenna gain, approximately 30 dBi, was available on the low band antenna. As the maximum plasma density (f_oF_2) in the F-region changed during these measurements, the ray bundle propagating to Shreveport increased in elevation angle while the VOA antenna beam was fixed. This means that the the caustic focusing region in the F-layer moved towards Delano and out of the heater beam while the E-region heating would be little affected by the same f_oF_2 changes. This systematic movement of the caustic region relative to Albuquerque is illustrated in Figure 11 as the MUF (2400) changes from 12.5 MHz to 15 MHz.

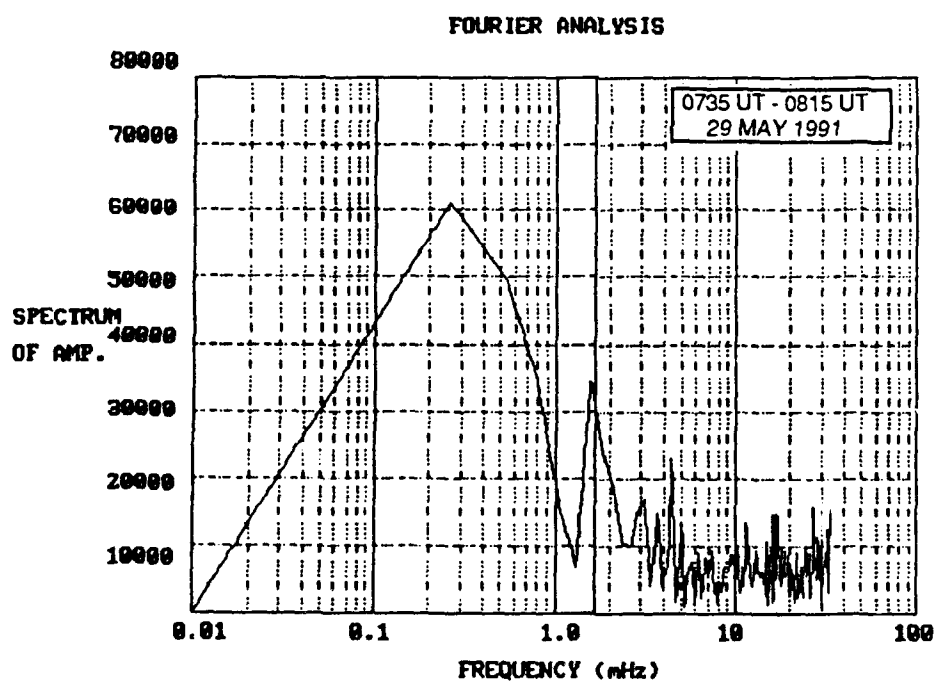
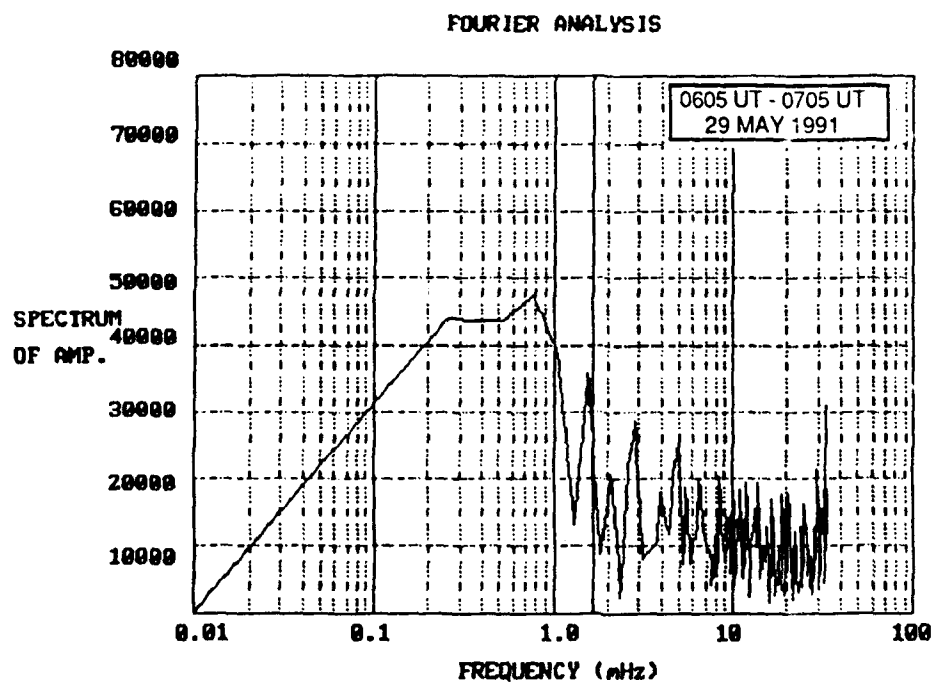


Figure 10. Fourier Spectra for the Selected Data Samples

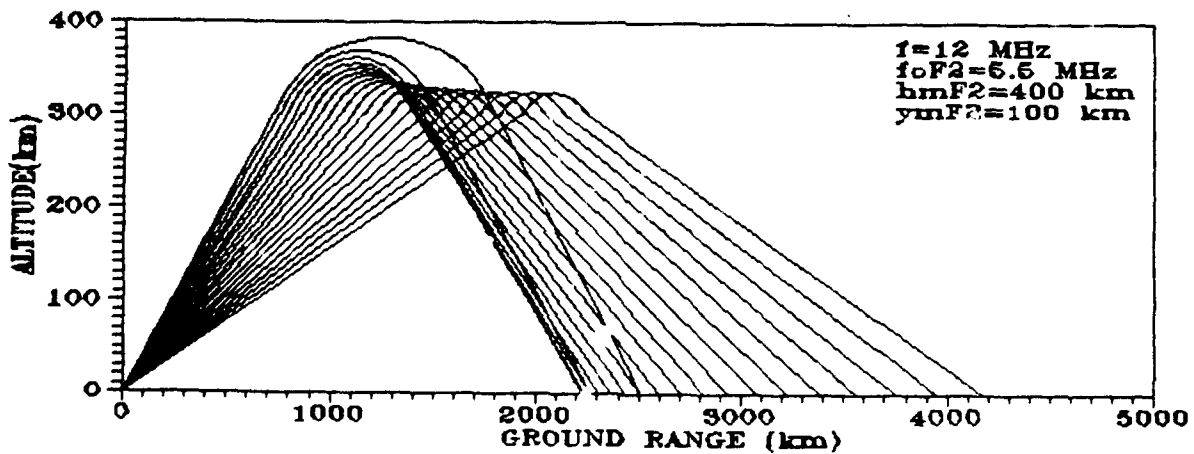
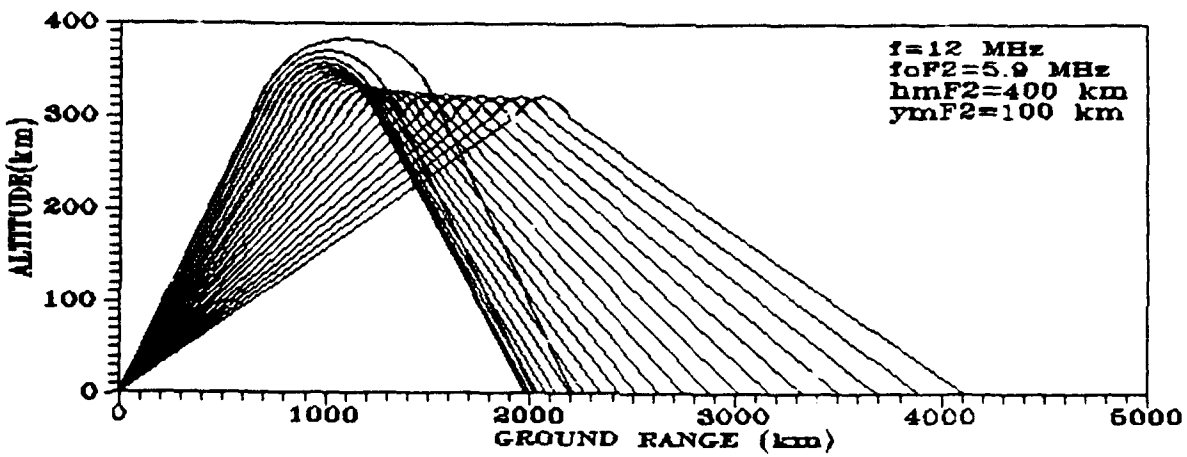
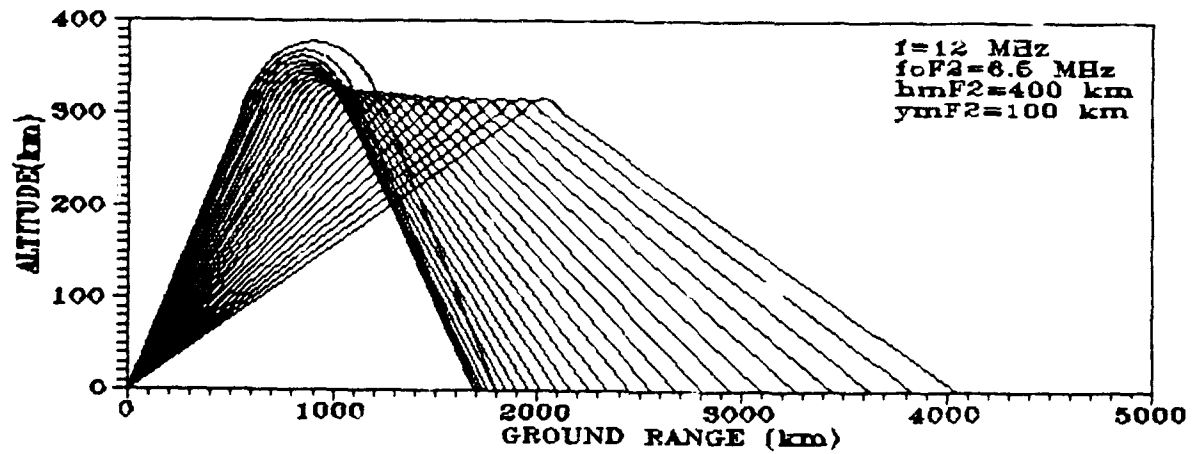


Figure 11. Ray Tracings Illustrating the Movement of the Caustic Region

Using these ray tracings, the movement of the skip caustic region, as the MUF changes relative to the heating frequency, is considered when estimating the local heater field strength. As the MUF increases, the skip caustic moves closer to the heater transmitter and out of the heater beam and the field strength in the caustic region decreases.

4.0 IONOSPHERIC HEATING

4.1 Introduction

Modification of the ionosphere by a high power (ERP between 85 and 90 dBW) HF communications system has been demonstrated. Ionospheric heating, i.e., heating of the constituents of the plasma, takes place through the transfer of energy from the high power radiowave to the electrons and positive ions. The electric field associated with the wave accelerates the charged particles in the plasma and these moving particles are able to retain the additional energy only after their motion has been disordered by a collision with another particle. It has also been assumed the applied electric field of the heater wave is of the form:

$$\vec{E} = \vec{E}_0 \exp(-j\omega t)$$

The equation of motion of an electron (neglecting the earth's magnetic field) in the applied electric field is then:

$$m \frac{d\vec{v}_e}{dt} = -e \vec{E} - m \nu_e \vec{v}_e \quad (1)$$

where ν_e is the electron velocity and ν_e is the electron-neutral collision frequency. Solving for the velocity, gives in phasor form:

$$\vec{v}_e = -\frac{e \vec{E}}{m} \left[\frac{\nu_e + j\omega}{\nu_e^2 + \omega^2} \right] \quad (2)$$

and changing to real quantities:

$$\vec{v}_e = - \frac{e \vec{E}_0}{m (\nu_e + \omega)} \left[v_e \cos \omega t + \omega \sin \omega t \right] \quad (3)$$

The average rate of increase of the electron energy, Q , is then:

$$Q = \frac{1}{T} \int_0^T \vec{v}_e \cdot (-e \vec{E}) dt = \frac{e^2 E_0^2}{2 m (\nu_e + \omega)} \nu_e \quad (4)$$

which is inversely proportional to the mass of the accelerated particle. The motion of the positive ions can be neglected since $m_i \approx 3 \times 10^4 m_e$, where m_i is the mass of the O_2 or N_2 ion and m_e is the mass of the electron. This available energy is transferred to the electrons and characterized as "heating" when the rate of collisions between the accelerated electrons and the dominant neutral species, O_2 and N_2 , is sufficiently large. This collision frequency, ν_e , depends on the energy of the electrons, expressed in terms of the mean temperature of the electron gas, and the number density of the neutral particles with which the electrons collide. The temperature dependent electron collision frequency (Gurevich, 1978) can be written as:

$$\nu_e = \nu_0 \left[\frac{T_e}{T} \right]^{\frac{5}{6}} \quad (5)$$

where ν_0 is the collision frequency when the electron gas is at the undisturbed temperature T and T_e is the heated electron temperature.

Energy is lost by the accelerated electrons because of the inefficiency of the collision process which transfers some of the acquired energy to the neutral particles. The fraction of the energy transferred, $\Delta E/E$, per collision is defined as δ . Gurevich discusses the range of δ , applying the kinetic theory for electrons and considering both elastic and inelastic type collisions. For elastic collisions, as would occur between electrons and atomic species in the atmosphere, e.g. atomic oxygen, δ is relatively small, of the order of 1×10^{-5} , while for molecular species where rotational and vibrational states can be excited, the collision process is inelastic and $\delta \approx 10^{-3}$. A full discussion of these collisional transfer processes is found in Gurevich (1978).

The rate of energy or heat loss is then proportional to δ and v_{em} and the energy (temperature) difference between the electrons and the neutral particles. This rate of heat loss, L , in terms of the electron temperature is:

$$L = \delta v_e k (T_e - T) \quad (6)$$

where k is Boltzmann's constant.

Combining the rate of energy gain and loss, the rate of change of the electron temperature is:

$$\frac{dT_e}{dt} = Q - L = \frac{e^2 E_o^2}{3 m_e k (v_e^2 + \omega^2)} v_e - \delta v_e (T_e - T) \quad (7)$$

The approximate steady state solution of this equation, i.e. where $dT_e/dt = 0$, gives for the new electron temperature relative to the ambient (neutral) temperature:

$$\frac{T_e}{T} = 1 + \frac{e^2 E_o^2}{3 m_e \delta k T (v_e^2 + \omega^2)} \quad (8)$$

The increased electron temperature, T_e , varies directly as the square of the electric field intensity E_o (which in turn is proportional to the ERP and inversely to the square of the distance from the transmitter to the heated region) and inversely as the square of the heater frequency.

To complete the analysis, the perturbed electron temperature is then used to calculate a modified electron density and collision frequency. For an oblique incidence transmitter with an ERP = 90 dBW (at 12 MHz), at an elevation angle of 12° (measured at the peak of the beam), the change in temperature relative to the ambient temperature for altitudes between 100 and 400 km is found in Table 1.

Table 1. Temperature Changes (%) vs. Altitude

<u>ALT(km)</u>	<u>$\Delta T_e/T$ (%)</u>
100	15
300	3.2
400	1.8

These percentage temperature increases were calculated by taking into account only the free space attenuation for the local field intensity. For F-region altitudes, these values are considered an upper bound because diffusion of the heated electrons has been neglected as an additional loss term. Diffusion reduces the heating effect in the F-region where the mean free path for the electrons is sufficiently large so that the "hot" electrons rapidly diffuse out of the heated region and are replaced by cooler ones from the surrounding areas. These calculated values for the F-region are reasonable, comparing them with the results of the more exact calculations by Bloom and Field (1989, c.f., Figure 5b, page 21). Depending on specific altitude, heating in the E-region is 4 to 8 time greater than in the F-region.

For the time variation of the electron density, N_e , it is necessary to consider the electron production rate caused by ionizing solar radiation and the electron loss rate by a dissociative recombination process. Here, the electron density variation is given as:

$$\frac{dN_e}{dt} = Q_e - \alpha N_e^2 \quad (9)$$

where Q_e is the ionization rate, α is the dissociative recombination rate and is proportional to both the temperature $T^{1/2}$ and the neutral particle density, N_m . The equilibrium electron density N_{eo} is then:

$$N_{eo} = \sqrt{\frac{Q}{\alpha}} \quad (10)$$

and here the nighttime equilibrium electron density varies with the temperature dependent recombination coefficient, which changes as a result of the electron heating. Because of the $T^{1/2}$ dependence, the change in the electron density is a small fraction of the change in the temperature given in Table 1. More importantly, for the IONMOD experiments, the time constant associated with the changes in the electron density is given as:

$$\tau_{N_e} = \frac{1}{\alpha N_e} \quad (11)$$

At night, in the F-region, $\tau_{N_e} \approx 3000$ s and in the E-region, $\tau_{N_e} \approx 2000$ s. These relatively large time constants for the change in the electron density means that with a five minute heating period, little change in electron density is expected.

These time constants must be compared with the time constants associated with the changes in temperature and collision frequency. From Equation 5:

$$\tau_{T_e} = \frac{1}{\delta v_{em}} \quad (12)$$

which is of the order of 10 ms in the E-region and 60 s in the F-region. The observed amplitude changes (see Section 2.1) appear to coincide with the heater-on time to within the 15 s sampling resolution. The rapid response indicates that E-region heating is the more likely location for the observed heating effects.

In the introduction to this report, two possible regions are considered where the heating process can take place at night. The first is in the F-layer in the vicinity of the caustic focusing region at 325 km, and the second is in the E-layer at an altitude around 100 km.

The work of Bloom and Field (1989) indicates, at night, only a very small change (a depletion of 1 or 2%) in the ambient electron density is possible in the F-region at an altitude around 250 km. For these May, 1991 IONMOD experiments, the peak of the F-layer was closer to 350 km and the reflection height for the oblique 12 MHz heater signal was above 300 km. At these altitudes the collision frequency is of the order of 100 to 200 s⁻¹ and it is not possible to significantly heat the electrons and confine them in a volume so that they affect the propagation of the probe signal. The several ray tracings presented by Bloom and Field for the case of nighttime F-region heating, show little or no amplitude change over most of the range behind the skip distance (Bloom and Field, 1989, Figure 7b); only a weak defocusing, of the order of 1 dB, for the very long distance rays (≈ 3000 km). The work of Field, et al. confirms the hypothesis that the heating cannot be in the F-region and an alternative explanation is presented.

4.2 Nighttime E-region Heating

Considering the above theory, the rate of change of the electron density after the turn-on of the heater is rather slow and it is only necessary to consider the variation of the collision frequency for heating periods of the order of 5 minutes. It is proposed that the observed amplitude changes are a result of increased absorption in

the E-region caused by an increase in the collision frequency. The absorption of a radiowave passing through a plasma depends both on the ambient electron density and the collision frequency.

The absorption of a wave passing obliquely through a slab of ionization of thickness Δz is given as:

$$\Delta A = \frac{N_e v_{em}}{2 \omega + v_{em}} \sec \theta \Delta z \quad (13)$$

where N_e is the electron density and θ is the angle the ray makes with the vertical. Then the total absorption through a region is:

$$A = \int_{z_1}^{z_2} \frac{N_e v_{em}}{2 \omega + v_{em}} \sec \theta dz \quad (14)$$

With the heating process, as discussed above, only the change in the collision frequency contributes to the change in the absorption of both the probe signal and the heater signal itself as it passes through the heated volume. As a first step towards a self-consistent solution, the differential absorption, Equation 13, is applied stepwise to the heater signal as it progresses to higher altitudes. This one way self-absorption of the heater signal is added to the free space loss considered earlier, to calculate the electric field in the next slab.

In addition to the normal nighttime E-layer, it is necessary to consider the effects of sporadic-E layers, particularly, since considerable Es was present during most of the nighttime operations. Figure 12 shows the Es scaled data using the vertical ionograms taken at the midpoint of the path. In fact, the vertical sounding site is considerably removed (about 700 km) from the VOA E-region intersection point, assuming a 12° elevation angle and a nominal 100 km height, i.e., about 400 to 500 km east of Delano. Considering the ionospheric heating model proposed here, future experiments would be better served by placing the sounder in the vicinity of the E-region intersection. Typically, the critical frequencies of the Es layers during

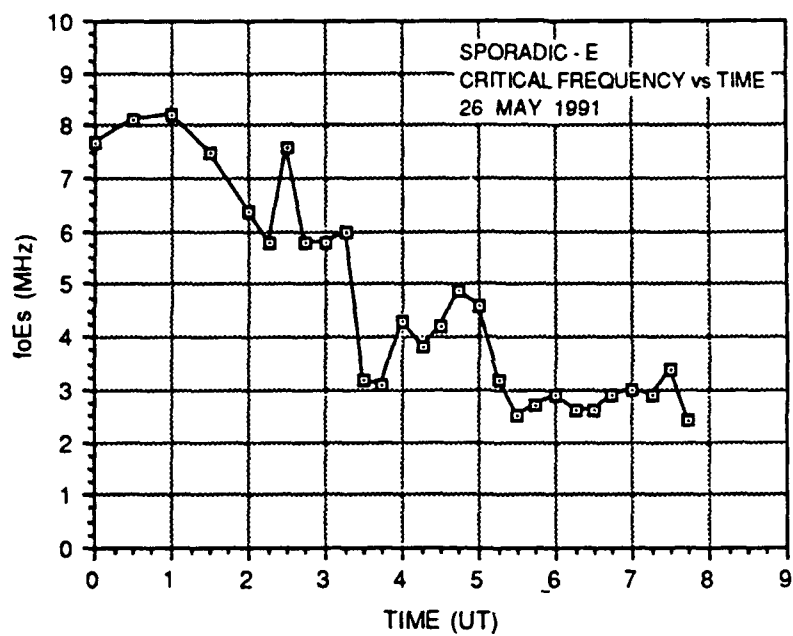


Figure 12. Scaled foEs and hEs for 26 May 1992

these experiments are around 3 to 4 MHz, though they often reach higher values. The height of the Es often appears to drop below 100 km. For comparison, measurements made using a rocket-borne mass spectrometer (Narcisi, 1971) shows a nighttime Es layered structure with a clear peak at 87 km and $f_oE_s = 2.2$ MHz.

For the current IONMOD experiments, the calculated increase in absorption of the probe signal at 12 MHz, using this E-region heating theory, for the normal nighttime E-layer, is very small, only 0.1 dB. Figure 13 shows the calculated increase in the absorption of the 12 MHz probe signal passing through the heated region, considering a parabolic Es layer (semi-thickness = 5 km) at altitudes between 85 and 105 km and critical frequencies from 1 MHz to 6 MHz. Here it is possible, realistically, to have up to 3 to 4 dB and even more additional absorption depending on the altitude and critical frequency of the Es layer in the vicinity of the ionospheric penetration point. Unfortunately, the available vertical soundings, because they are in the wrong location, cannot be directly correlated with the observed periods when the probe amplitude changes were observed.

5.0 SUMMARY

It has been shown that E-region heating, at altitudes around 100 km, is possible at night, though at 12 MHz and 12° elevation angle, at 90 dBW, a sporadic-E layer with higher electron density is required. In the E-region, the maximum nighttime electron density is $N_e = 5 \times 10^9 \text{ (m}^{-3}\text{)}$ at around 105 km for the E-layer and up to $2 \times 10^{11} \text{ (m}^{-3}\text{)}$ for sporadic-E layers. The collision frequency varies from $4 \times 10^4 \text{ (s}^{-1}\text{)}$ to $2 \times 10^5 \text{ (s}^{-1}\text{)}$ over the range of E-region altitudes. Under these conditions, there are sufficient collisions to alter the velocity distribution of electrons subject to a strong applied electric field and this redistribution of the velocities is described in terms of an increase in the mean electron temperature.

In the heated plasma, N and ν , are dependent on the electron temperature. Under equilibrium conditions, the electron density depends, inverse'y on the fourth root of the temperature because the dissociative recombination rate decreases as the electron temperature increases. For the electron-neutral collision frequency, the increased electron temperature increases the rate of collisions. Together, the product $N\nu$ tends to become larger in the heated region and the absorption of any

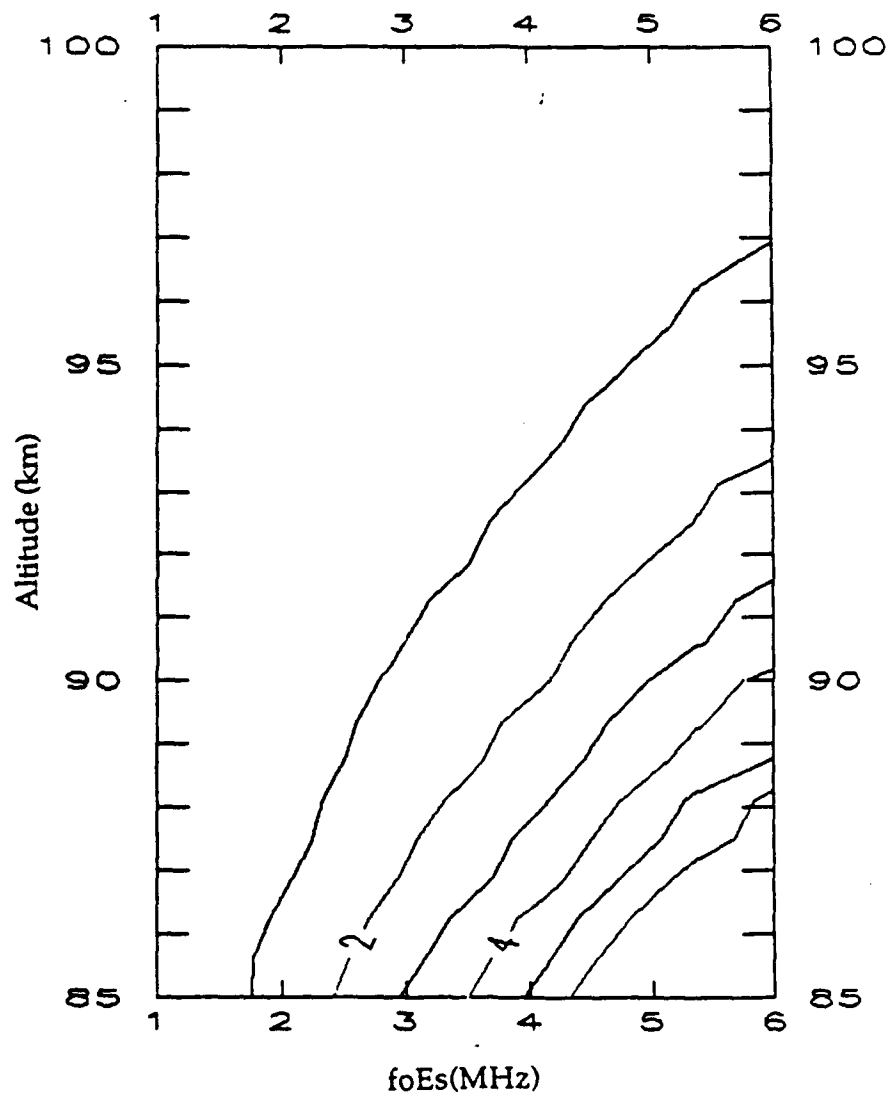


Figure 13. Increased Absorption for Sporadic-E Ionization (Night)

radiowave passing through the heated E-layer patch, including the heater signal and the probe, increases. Using simple geometry for the antenna beamwidth, the VOA heater transmitter produces a heated patch about 50 km wide by 400 km long, though it is not uniformly illuminated; the higher field intensities and the more strongly heated areas are located closer to the Delano end of the patch.

To determine the increase in electron temperature, the heater field strength ($E_0 \approx 500$ mV/m for a 90 dBW system at 12° elevation) at E-region altitudes must be compared to the characteristic plasma field intensity, E_p ;

$$E_p = \frac{e^2}{3 k T m_e \delta \omega^2} \quad (14)$$

as defined by Gurevich (1978). This characteristic field is estimated to be around 1500 mV/m at 12 MHz and 200° K, though, there is some uncertainty for the value of δ in a weakly ionized ionospheric plasma where the atomic and molecular species varies and the distribution of electron velocities \bar{v} is likely to be non-Maxwellian. The estimation of the parameters T and δ which define E_p is sensitive to the detailed shape of the velocity distribution function. In the situation studied here, the presence of sporadic-E seems to be important indication of non-stationary conditions that also affects the degree of electron heating.

Using the characteristic plasma field calculated above as an upper limit, and including moderate sporadic-E, it is possible to account for observed increase in probe signal absorption. Based on Gurevich's work, the required rate of energy transfer, δ , lies between the value for elastic collisions and the one for inelastic collisions, where a fraction of the electron energy is transferred to the neutrals through the collisional excitation of rotational and vibrational states in the neutral molecules.

Finally, the time constants associated with the changes in the electron temperature and collision frequency were found to be very short, of the order of tens of milliseconds or less while for the electron density changes, the time constants are of the order of tens of minutes. For this reason, the additional absorption results only

from a change in the collision frequency and this helps explain why no changes in the probe signal elevation angle or Doppler frequency were observed when the heater was turned on. To the extent that Es is important at night, it is easy to understand why the observed heating events appear to occur somewhat erratically.

Future work is planned to put the theory of E-region heating on a more quantitative and self-consistent basis. This includes E-region dynamics with drift motions, gravity waves and the presence of sporadic-E. Little supporting data is available for predicting the normal nighttime E-layer structure and models for the electron production and loss mechanisms (Keneshea et al., 1970), combined with the dynamics are required to understand and predict the effect of normal variations in the night electron density on the performance of high power radio systems. The entire IONMOD data base needs to be examined using the analysis techniques developed here to determine those periods when heating was effective and under what ionospheric conditions these changes occurred. This examination includes the data collected during the daytime experiments where D-region heating must also be considered.

REFERENCES

Field Jr., E.C. and R.M. Bloom, Ionospheric Heating with Oblique Waves, Pacific Sierra Report # 1864, August, 1989.

Gurevich, A.V.; Nonlinear Phenomena in the Ionosphere, Springer-Verlag, 1978

Keneshea, T.J. and M.A. McLeod, Wind Induced Modification of E-region Ionization Profiles, J. Atmos. Sci., 27, 981-984, 1970.

Narcisi, R.C., Composition Studies of the Lower Ionosphere, Physics of the Upper Atmosphere, Bologna, 1971.

Sales, G. and I. Platt, High Power Oblique Incidence HF Ionospheric Modification, GL-TR-90-0078, April, 1990, **ADA224402**